

CANDOCK: Chemical atomical network based hierarchical flexible docking algorithm using generalized statistical potentials

Jonathan Fine^{1, ‡}, Janez Konc^{2, ‡}, Ram Samudrala³, Gaurav Chopra^{1,4,5,6,7 *}

¹Department of Chemistry, Purdue University, 720 Clinic Drive, West Lafayette, IN 47906

²National Institute of Chemistry, Hajdrihova 19, SI-1000, Ljubljana, Slovenia

³Department of Biomedical Informatics, SUNY, Buffalo, NY, USA

⁴Purdue Institute for Drug Discovery

⁵Purdue Center for Cancer Research

⁶Purdue Institute for Inflammation, Immunology and Infectious Disease

⁷Purdue Institute for Integrative Neuroscience

[‡]These authors share equal contribution to this work.

*Corresponding Author

E-mail: gchopra@purdue.edu

Abstract

Small molecule docking has proven to be invaluable for drug design and discovery. However, existing docking methods have several limitations, such as, ignoring interactions with essential components in the chemical environment of the binding pocket (e.g. cofactors, metal-ions, *etc.*), incomplete sampling of chemically relevant ligand conformational space, and they are unable to consistently correlate docking scores of the best binding pose with experimental binding affinities. We present CANDOCK, a novel docking algorithm that utilizes a hierarchical approach to reconstruct ligands from an atomic grid using graph theory and generalized statistical potential functions to sample chemical relevant ligand conformations. Our algorithm accounts for protein flexibility, solvent, metal ions and cofactors interactions in the binding pocket that are traditionally ignored by current methods. We evaluate the algorithm on the PDBbind and Astex proteins to show its ability to reproduce the binding mode of the ligands that is independent of the initial ligand conformation in these benchmarks. Finally, we identify the best selector and ranker potential functions, such that, the statistical score of best selected docked pose correlates with the experimental binding affinities of the ligands for any given protein target. Our results indicate that CANDOCK is a generalized flexible docking method that addresses several limitations of current docking methods by considering all interactions in the chemical environment of a binding pocket for correlating the best docked pose with biological activity.

1. Introduction

Computational docking provides a means to predict and assess interactions between ligands and proteins with relatively little investment. Application to proteins involved in disease holds the promise of discovering new drug therapeutics. After decades of method development and application, this promise has not been fully realized. The CANDOCK algorithm confronts several outstanding technical and practical problems in computational docking. One significant problem is assessing goodness-of-fit, or the likelihood that the given pose is the most physically realistic (native-like) pose among many unrealistic binding poses. Another significant limitation is the lack of full protein flexibility in the docking methods used today. The induced fit is a widely recognized challenge in computational drug screening, where the protein and the ligand undergo conformational changes upon ligand binding. Therefore, the traditional treatment of proteins as rigid structures is insufficient and often misleading for structure-guided drug screening and design. Docking ligands to their protein targets is particularly challenging when attempting to reproduce the binding mode of small molecules to ligand-free or alternative ligand-bound protein structures, which invariably occurs in the practical application of any docking method. Specifically, docking with ligand-bound (holo) protein structures typically leads to an accuracy of 60-80%, whereas ligand-free (apo) structures yields a docking accuracy of merely 20-40%¹⁻⁵.

Several methods have been implemented to account for protein and ligand flexibility, including multiple experimentally derived structures from X-ray crystallography⁶, nuclear magnetic resonance⁶ rotamer libraries^{7,8}, Monte Carlo^{9,10}, and molecular mechanics^{11,12}. The same principle limits use of multiple experimentally derived protein structures or side-chain rotamer libraries: binding a ligand to a protein can cause conformational changes in either molecule that are not captured by these methods¹³.

The sampling problem is compounded by the fact that the protein main chain torsion angles are also frequently altered from their ligand-free conformations, which these methods fail to capture.

Molecular mechanics is well suited for capturing fine detail side-chain and main chain motions and rearrangements through energy minimization. However, molecular mechanics is limited in that adequate sampling of all degrees of freedom between protein and ligand: rotation, translation, and torsion angle are frequently computationally intractable. Further, the use of molecular dynamics has been shown to disrupt the ligand from its native pose¹⁴.

Modern docking methods address these issues by employing algorithms such as the Genetic Algorithm¹⁵⁻¹⁸ to sample the conformational space flexibly. However, it has been shown that these methods do not adequately produce poses that rank the activity of the ligand well^{17,19} and that the ability of these methods to produce a correct pose is dependent on the starting conformation of the ligand in question^{20,21}. Some methodologies use a fragment-based approach to docking²² to sample the conformational space for a given ligand efficiently. These fragment-based methods have reported a greater ability to rank activity between given ligands^{23,24}. Therefore, we believe that further expansion of fragment-based approaches is an appropriate way to improve upon previous works.

We have developed the CANDOCK algorithm around a new protocol for hierarchical docking with iterative dynamics during fragment reconstruction. The docking protocol is based on two guiding principles: (i) binding sites possess regions of both very high and very low structural stability²⁵ and (ii) small protein motions are generally sufficient to predict the correct binding mode of protein-ligand interactions¹³. The hierarchical nature of this method is derived from an ‘atoms to fragments,’ ‘fragments to ligands’ approach that generates all chemically relevant poses given the ligand and surrounding protein binding site. The expectation is that, regardless of whether we begin with a holo or apo protein structure, at least one or a few fragments derived from a flexible ligand will bind to a structurally stable region of the protein. Following identification of such a binding mode, subtle conformational changes necessary for reconstructing the ligand using these fragments as seeds will be captured by molecular mechanics energy minimization. We show that CANDOCK can reproduce the binding mode of ligands in holo proteins and rank the activity of these ligands using a knowledge-

based forcefield.

2. Materials and methods

2.1. Generalized statistical scoring function

A generalized statistical scoring potential is used to account for varying chemical environments, such as metal ions, cofactors, water molecules, *etc.* The scoring function employed by the CANDOCK algorithm is a pairwise atomic scoring function that is based on the work carried out by Bernard and Samudrala²⁶. Here we reproduce the fundamental equations developed in Ref. 26 to clarify the terminology used in the present work. The scoring function calculates the potential between two atoms based on the distance between atoms i and j with atom types a and b and takes four input terms that determine the method by which score is calculated. The possible terms are ‘functional’, ‘reference’, ‘composition’, and ‘cutoff’. They define the function P given in the basic Eq. (1):

$$S(r_{ab}^{ij}) = - \sum_{ij} \ln \frac{P(r_{ab}^{ij} \vee C)}{P(r^{ij})} \quad (1)$$

The ‘functional’ term controls the numerator of Eq. (1) and can be defined as a ‘normalized frequency’ function $f(r)$ in Eq. (2)

$$P(r_{ab}^{ij} \vee C) = f(r_{ab}) = \frac{N_s(r_{ab})}{\sum_r N_s(r_{ab})} \quad (2)$$

where N_s is the number of observed atoms found at a given distance. Alternatively, it can be defined as a ‘radial’ distribution function $g(r)$ in Eq. (3)

$$P(r_{ab}^{ij} \vee C) = g(r_{ab}) = \frac{\frac{N_s(r_{ab})}{V_s(r)}}{\sum_r \frac{N_s(r_{ab})}{V_s(r)}} \quad (3)$$

where N_s is divided by the volume of the sphere $V_s(r)$. To distinguish between these two functions, ‘radial’ scoring functions start with ‘R’ while ‘normalized frequency’ functions start with ‘F.’

The ‘reference’ term determines the denominator of the scoring function. It can be defined either as ‘mean’, in which case it is calculated as a sum of all atom type pairs divided by the number of atom types. This term can be used with either ‘normalized frequency’ (Eq. (4)) or ‘radial’ (Eq. (5))

$$P(r) = f(r) = \frac{\sum_{ab} f(r_{ab})}{n} \quad (4)$$

$$P(r) = g(r) = \frac{\sum_{ab} g(r_{ab})}{n} \quad (5)$$

The second option is the ‘cumulative’ which denotes cumulative distribution. Used together with ‘normalized frequency’ this yields Eq. (6) and ‘radial’ yields Eq. (7).

$$P(r) = f(r) = \frac{\sum_{ab} N_s(r_{ab})}{\sum_r \sum_{ab} N_s(r_{ab})} \quad (6)$$

$$P(r) = g(r) = \frac{\sum_{ab} \frac{N_s(r_{ab})}{V_s(r)}}{\sum_r \sum_{ab} \frac{N_s(r_{ab})}{V_s(r)}} \quad (7)$$

Scoring functions compiled with the ‘mean’ option are denoted as ‘M’ while those compiled with the ‘cumulative’ are denoted as ‘C.’ The third term defines the composition of the scoring function. This term controls the number of unique atom pairs used for compiling the scoring function. The ‘complete’ option will result in the scoring function compiled from all possible atom type pairs while the ‘reduced’ option will result in only atom pairs possible in the given complex to be used. The letter ‘C’ is used to denote complete scoring function while ‘R’ is used to denote scoring function that is compiled with

the ‘reduced’ option. In total of 8 scoring function families can be created with these three options. The fourth and final term used to compile the scoring function is the ‘cutoff’. This controls the maximum distance at which the interactions will be calculated, the possible values ranging from 4 Å to 15 Å. With all four options there are a total of 96 possible scoring functions (8*12). Example scoring functions are ‘radial-mean-reduced-6’ (RMR6) and ‘normalized frequency-cumulative-complete-8’ (FCC8).

2.2. Phase I: Structure Preparation

The CANDOCK algorithm takes as input a set of compounds to be docked, a query protein structure, and a set of binding sites on the query protein structure. In a three-phase protocol (**Figure 1**), it performs semi or fully flexible docking of compounds to the protein and outputs docked and minimized protein-compound complex structures together with their predicted scores.

2.2.1. Parse receptor and compounds. The input to the algorithm are the 3D coordinates and topology of a query protein structure consisting of single or multiple chains which may also contain cofactors and post-translation modifications in the PDB format, and compounds in MOL2 format. Compounds are processed in batches of size 10 to enable reading of large molecular files that do not fit in computer memory. An example of a ligand is given in **Figure 2a**.

2.2.2. Compute atom types. To compute atom types for protein, cofactors, and compounds, we implemented the IDATM algorithm²⁷ (results given in **Figure 2b**). We also implemented an algorithm^{28,29} to assign AMBER General Force Field (GAFF) atom types to cofactors, ligands, and post-translational modifications, while GAFF types for proteins are obtained from the AMBER10 topology file available as part of the OpenMM package³⁰

2.2.3. Assignment of bond orders. Using the hybridization information provided by the newly assigned IDATM atom types, several potential bond order states can be generated as to fit with the expected number of bonds (valence) for each ligand atom. These potential bond order assignments are

evaluated in a trial and error fashion to determine whether they form a valid molecule using valence state rules derived for all atom types. The bond order set that satisfies all the requirements (see **Figure 2c**) for is used to assign GAFF bond orders to the ligand.

2.2.4. Fragment compounds. Rotatable bonds are first identified in each compound using the extended list of rotatable bonds adapted from the UCSF DOCK 6 software³¹. Next, structurally rigid fragments consisting of atoms between the rotatable bonds are identified. Bond vectors for rotatable bonds are retained for each rigid fragment to be used during reconstruction of docked fragments. Fragments consisting of more than 4 atoms, in which at least two atoms are rigid, that is, are connected by a non-rotatable bond, are considered as seed fragments. These are subsequently rigidly docked into the protein binding site. All other non-seed fragments are considered as linking fragments during the compound reconstruction process. This result is shown in **Figure 2d**.

2.2.5. Assignment of force field atom types. Using the computed GAFF atom types, the bonded forces of the AMBER force field are generated for the protein and the docked compounds. Protein-compound interactions are scored using the knowledge-based Radial Mean Reduced (RMR) discriminatory function of Bernard and Samudrala²⁶ with a 6 Å cutoff (see section Knowledge-based scoring function). This function calculates a fitness score for each compound's or fragment's atom in a protein by considering all protein atoms within 6 Å radius of that atom. It is an atomic level radial distribution function with mean reference state that averages over all pairwise atom types from a reduced atom type composition (protein's and compound's atom types), using experimentally determined intermolecular complexes in the Cambridge Structural Database (CSD)³² and in the Protein Data Bank (PDB)³³ as the information sources.

The objective function that is used for the minimization of the protein-compound interactions is computed using the RMC scoring function with a 15 Å cutoff as follows: for each possible pair of atom types present in the protein-ligand complex, the RMC function is sampled at discrete 0.1 Å intervals and is smoothed using B-spline interpolation. Potential energy values and their first derivatives are

calculated at 0.01 Å intervals over the [0, 15] Å interval for the smoothed function. The objective function is implemented as a custom knowledge-based force object in OpenMM³⁰ which is used as a library from the CANDOCK source code.

2.2.6. Prepare protein for molecular mechanics. The N- and C- terminal residues are renamed according to the AMBER topology specification, e.g., ALA to NALA or CALA, disulfide bonds are added to the protein by connection of SG atoms that are closer than 2.5 Å, inter-residue bonds are also added by connection of main chain C and N atoms that are closer than 1.4 Å.

2.3. Phase II: Rigid Fragment Docking

2.3.1. Compute rotations of seeds. For each seed fragment, we compute its rotational transformations about the geometric center which is fixed at the coordinate origin. Accordingly, we first compute 256 uniformly distributed unit vectors around the coordinate origin. Then, the seed fragment is rotated by 10° increments around the axis formed by each unit vector. To speed up the subsequent step of rigid fragment docking, the rotated fragment atoms' coordinates are mapped on a hexagonal close-packed (HCP) grid of 0.375 Å resolution. This mapping enables efficient docking of fragments to a protein binding site since their rotational transformations need to be computed only once. The fragment's clashes with the protein and the fragment's RMR6 scores are determined by translations of the rotational fragment grid over the compatible HCP binding site grid using fast integer arithmetic.

2.3.2. Generate binding site grid. A binding site location for docking is specified using one or more centroids, each consisting of the Cartesian coordinate of its center and its radius. We generate a binding site grid that covers the space of all centroids that represent the binding site (**Figure 3a**). We use an HCP grid that provides maximal packing efficiency, covering the same volumetric space of a simple cubic grid with approximately 40 % fewer grid points to achieve the same maximal interstitial spacing. The grid points are in a distance range of $0.8 \text{ \AA} < d < 8 \text{ \AA}$ from any protein atom. We use a grid spacing of 0.375 Å with a maximal interstitial spacing of 0.22 Å to densely represent the protein binding sites

(Figure 3b).

2.3.3. Dock and cluster rigid fragments. Intermolecular geometric and chemical complementarity between a protein and a ligand is essential for binding. Energetically preferred positions of ligand atom types can be captured using a discriminatory function (Figure 3c). Docking of seed fragments to the binding site grid is performed by moving seed's rotational grid over the binding site grid points. Docked fragment poses that are in a steric clash with the protein are rejected (Figure 3d). A steric clash is considered if any interatomic distance between the fragment and the protein falls within nine-tenths of the atoms' respective van der Waals sum. Each fragment translation and rotation that passes this initial filter is then evaluated with the RMR6 discriminatory function²⁶. Finally, greedy clustering of docked and scored fragment poses in the Root Mean Square Deviation (RMSD) space computed based on their heavy atoms at 2 Å cluster cutoff is performed, resulting in a uniform distribution of locally best-scoring docked seed fragments covering the entire protein binding site (Figure 3e).

2.4. Phase III: Flexible docking with iterative minimization

2.4.1. Generate partial compound conformations. For each compound to be docked, a user-specified percentage of each of its best-scoring rigidly docked seed fragment poses are considered. Among these, we search for such compatible pairs of docked seeds that are at the appropriate distances, that is, the distance between them is less than the maximum of their known bond distance. The maximum possible distance between a pair of seeds is calculated by traversing the path between the fragments in the original compound and summing up the distances between the endpoints of each rigid fragment on the path.

We construct an undirected graph in which vertices represent seed fragments, and edges indicate that the corresponding pair of seed fragments is linkable. Using the MaxCliqueDyn algorithm of Konc and Janezic³⁴, we then find all fully connected subgraphs consisting of k vertices (k -cliques) in this graph, where the default value of k is set to three or to the number of seed fragments, whichever

value is less. Each k-clique corresponds to a possible partial conformation of the docked seed fragments, in which these fragments are appropriately distanced so that they may be linked into the original compound. The possible partial conformations are then clustered using a greedy clustering algorithm at RMSD cutoff of 2 Å, where the best-scored cluster representatives are retained. The partial conformations sorted by their RMR6 scores from the best- to the worst-scored are used as an input to the next step of compound reconstruction.

2.4.2. Reconstruct compound with protein flexibility. Each identified partial conformation of the docked seed fragments is gradually grown into the original ligand by addition of non-seed fragments using the A* search algorithm. This can be done at different levels of protein flexibility. Protein minimization may be performed at each step of the linking process or only at the end when the compound has been reconstructed. Each seed fragment is linked to adjoining fragments according to the connectivity of the original compound. Each added non-seed fragment is rotated 360° about the bond vector at 60° increments. If the user has specified full protein flexibility, the resulting conformation of the partial compound and the protein is subjected to knowledge-based energy minimization using the RMC15 scoring function as for intermolecular forces. Simultaneously, bonds, angles and torsions of the partial compound and the protein are minimized using the standard AMBER molecular mechanics energy minimization. This procedure uses the popular OpenMM software package, specifically its implementation of the L-BFGS minimization algorithm³⁵. With each round of minimization, the RMR6 score is calculated for the protein-compound interactions, and the scored conformation is added to the priority queue which consists of the growing compound conformations in the order from the best-scored to the worst-scored.

At each subsequent step of reconstruction, the A* search algorithm chooses the best-scored conformation from this priority queue and attempts to extend it. This conformation must meet an additional condition, which is that its attachment atoms that are to be connected by rotatable bonds to fragments not-yet added, need to be at appropriate distances from the attachment atoms on the

remaining seed fragments. The algorithm iterates until the priority queue is empty in which case the compound has been completely reconstructed and is in a local minimum energy state. Alternatively, if the specified maximum number of steps was exceeded (1000 by default), then the reconstruction failed. The A* search is repeated for each partial conformation of docked seed fragments until all have been considered for reconstruction into a different docked conformation of the original compound. A final energy minimization procedure is performed on the protein-ligand complex treating the protein as fully flexible (side-chain and backbone) to remove steric clashes in the process of growing the ligand into the binding site. In addition to knowledge-based and molecular mechanics energy minimization, the fragment reconstruction process intrinsically accounts for ligand flexibility in the docking process. The described protocol results in a ranked list of docked and minimized protein-compound complexes.

2.5. Benchmarking the CANDOCK algorithm

2.5.1. *Benchmarking set of choice.* We benchmarked the CANDOCK hierarchical docking algorithm using a benchmarking set (1) to determine whether the algorithm can reproduce the crystal binding pose of the ligand in the binding site of the protein and (2) to correlate the scores of the three-dimensional (3D) docked poses of the ligand to the measured K_d/K_i values of the ligand binding with the protein. PDBbind benchmark³⁶ is very well suited for this analysis because, for each protein in this set, it provides 3D coordinates and corresponding activity values for five protein-ligand complexes. In the PDBbind v2016 core set, there are a total of 285 such complexes for 57 proteins of interest to the medicinal chemistry community. The number of fragments present in a given ligand range from a single fragment to ligands consisting of thirteen fragments, enabling an evaluation of our method on both rigid and flexible ligands.

In addition to PDBbind, we have also benchmarked our method against the Astex Diverse set³⁷ as several protein-ligand complexes in this set include metal ions and other cofactors, allowing us to showcase these examples and how our algorithm handles these particular cases. We obtained each

structure from the Astex set from the Protein Data Bank directly and only considered the biological assembly used to create the original benchmark.

2.5.2. Input preparation. The binding site for both benchmarking sets is defined by spheres with a radius 4.5 Å centered around each atom of crystal ligand. We did not remove any cofactors, solvent molecules, ions, or glycans when preparing our docking runs. The provided reference ligand was used to generate fragments and seeds for docking.

2.5.3. Parameters chosen for benchmarking. The most important parameter present in CANDOCK for linking seeds into ligands is the ‘Top Percent’ parameter which is crucial to selecting the number of seeds used to generate potential conformations via the maximum clique algorithm. If this number is too small, then there will not be enough potential conformations generated to sample the conformational space of the ligand properly. In fact, there is a possibility that no conformations are generated during the linking step, causing CANDOCK to fail to produce any conformations. If the ‘Top Percent’ is too large, then the conformational search space is too large, and CANDOCK will become computationally inefficient (especially in the case of fully-flexible protein docking). Therefore, we wanted to sample potential ‘Top Percent’ values to determine how well our method does at various levels of conformational space sampling. The values chosen for this parameter are 0.5%, 1.0%, 2.0%, 5.0%, 10%, 20%, 50%, and 100%.

Similar to the conformational space sampled, we also investigated the effect of protein flexibility on the ability of the CANDOCK algorithm to reproduce the binding pose of a ligand. Accordingly, we used the algorithm in three modes: no protein flexibility (no energy minimization performed), with semi-flexible protein (final energy minimization only), and with a fully flexible protein (iterative energy minimization performed). The RMSDs for all poses generated from all ‘Top Percent’ values and all flexibility modes are calculated with respect to the experimental crystal pose using a symmetry independent method.

Finally, we wished to determine the best scoring function to select the crystal pose from all

generated poses (the ‘selector’ scoring function’) and potentially differentiate it from the scoring function used to rank the activity of a given ligand to the protein target of interest (the ‘ranker’ scoring function). To do this, we calculated the score of all poses generated for the PDBbind core set using all scoring functions mentioned in section 2.1. We then evaluated the ability of each scoring function to select the crystal pose of a ligand from all poses as well as the correlation between the score assigned to the selected pose and the experimental binding affinity. As there are 96 scoring functions, there are 9216 (96 ways to select*96 ways to rank) different methods to rank the affinity of the ligands in the PDBbind core set. An overview of this benchmarking process for activity prediction is given in **Figure S9**.

3. Results and discussion

Herein we discuss the performance of the CANDOCK algorithm in reproducing the crystal pose of a ligand via sampling the conformational space of the ligand in the binding pocket modeled with different levels of protein flexibility for two benchmarking sets. In addition, we evaluate the ability of the algorithm to discriminate the crystal pose from the all poses generated by the algorithm, and the ability to rank the activity of the ligands against the protein targets of interest.

3.1. CANDOCK provides stellar conformational sampling of a ligand in the protein binding site with large values of the ‘Top Percent’ parameter

The most important feature of a flexible ligand docking methodology is its ability to produce a ligand pose within 2.0 Å of the crystallized pose of the ligand. Since our methodology has inherent ligand flexibility due to its hierarchal nature, we evaluate its ability to produce ligand poses both near and far from the native crystal pose of the ligand regardless of the score of the ligand pose. At this stage we wish to investigate if a single “good” pose is present among the docked poses. The plots of RMSD values generated indicate that our algorithm adequately samples the conformational space of the ligands in the PDBbind Core set (**Figure S1**). Their Boltzmann-like distribution indicates that

conformations both far from, and close to the ligand pose are sampled.

To validate our docking procedure, we have plotted the best RMSD for all protein-ligand complexes as well as the RMSD for the best-scored pose as the cumulative frequency for all ‘Top Percent’ values and varying degrees of protein flexibility in the left-hand panels of **Figure 5**. These plots indicate that the use of larger ‘Top Percent’ values such as 20%, 50%, and 100% produce more poses within 2.0 Å than lower ‘Top Percent’ values (0.5% - 10%). For the semi-flexible (**Figure 5c**) method, the ‘Top Percent’ value of 20% yielded the greatest number of poses within 2.0 Å of the crystal pose. The success rate, ability to produce at least one “good” pose, at this value is 91%. If one considers all ‘Top Percent’ values investigated, the overall success rate of the semi-flexible method is 94%. Excluding the three peptides present in PDBbind (which are generally ignored in docking studies), there are only 12 co-crystals where CANDOCK fails to find a single “good” pose.

Although full protein flexibility (**Figure 5e**) is not required to achieve the best number of correct poses for these large ‘Top Percent’ values, the fully flexible protein method outperforms the semi-flexible (**Figure 5c**) and rigid protein (**Figure 5a**) methods for smaller ‘Top Percent’ values such as 10% and 5%.

These results indicate that hierarchical generation of poses is a successful strategy for sampling the conformational space of ligands in protein-ligand complexes when protein flexibility is only considered after pose generation.

3.2. The Radial Mean Reduced scoring function is best for selecting the ligand pose

The right-hand panels of **Figure 5** give the selection rate, which is defined as the ability to select a pose within 2.0 Å from all poses generated by the algorithm. The RMR6 scoring function performs best for the semi-flexible method and the best selection scoring function for the rigid protein case (RMR8) and the fully-flexible protein case (RMR5) are both of the same type (RMR) and have similar cutoffs of 8 Å and 5 Å, respectively. Conversely, the RCC family of scoring functions performs the worst in

selecting the crystal pose from the generated poses. The RCC11 scoring function is the worst in this family and can be used as an example of a bad selector.

To elucidate the rationale behind the performance of RMR6 in selecting a good pose we plotted the RMR6 of the pose with the smallest RMSD against the score of the crystal pose in **Figure S3-5**. For ‘Top Percent’ values greater than 10%, there is a clear separation between the poses within 2.0 Å and the poses far from the crystal pose (failures). These failures cluster above the identity line, indicating RMR under-scores these complexes during sampling. Since these cases are rare, it is best to evaluate them on a per ligand basis, which we do in the following section.

3.3. CANDOCK does not perform well with compounds containing long chains of aliphatic carbons

Examining the failures of a method to produce the desired outcome can illuminate potential issues with the algorithm and can be used to address these problematic areas in the future. In the case of CANDOCK, only 12 out of the 285 protein complexes in PDBbind proved to be complete failures, that is, no combination of method and ‘Top Percent’ could yield a predicted pose within 2.0 Å of the crystal pose. Of these 12, six complexes (1H22, 1H23, 3AG9, 3KWA, 3UEU, and 4EA2) contain an aliphatic carbon chain greater than 4 atoms. This is significant as the fragmentation of ligands does not consider aliphatic chains to be fragmented and uses a separate strategy for determining the location of linkers in these molecules and therefore have a high ratio of rotatable bonds to ligand fragments. Also, aliphatic chains consist of the same atom type (sp³ hybridized carbon; C3) repeated in 3D space. We plan on addressing this issue in later versions of CANDOCK by using a different sampling method and ligand-class specific scoring function, similar to what was done for the support of carbohydrates in Autodock Vina³⁸.

3.4. Full protein flexibility is vital for protein-ligand complexes with a large number of rotatable bonds

A critical feature of a scoring function is its ability to identify the binding pose of a ligand successfully. It has been previously shown that the number of rotatable bonds in a ligand significantly influence the ability of a scoring function to select the best RMSD value for a given complex⁵. Since the number of ligand fragments is more indicative of CANDOCK's performance due to its fragment-based nature, we present the selection rate of the RMR6 scoring function as a function of the number of fragments in a ligand (**Figure 6**). Recall that the selection rate is defined as the percentage of the docked poses within 2.0 Å of the native ligand among the n top-ranked poses. Comparison of **Figure 6c** (fully-flexible) to **Figure 6a** (semi-flexible) and **Figure 6b** (semi-flexible) reveals that the selection rate for ligands with more than 6 fragments increases as the flexibility increases.

For ligands with 6 or fewer fragments, the semi-flexible (**Figure 6b**) and fully-flexible (**Figure 6c**) methods perform similarly well. Thus, there is no need for full-protein flexibility for smaller ligands. This is most likely caused by the plateauing of generated poses for ligand with >5 fragments for 'Top Percent' values greater than 10% (**Figure S2**). This plateau means there is an upper limit to the sampling space possible for a given binding site and once this threshold is reached, the algorithm is no longer able to produce enough poses. The increased flexibility allows this methodology to maneuver the ligand into its binding pose, leading to a greater selection rate.

3.5. CANDOCK is able to generate native-like poses for complexes in the Astex Diverse set

The Astex Diverse Set³⁷ is another popular benchmarking set for measuring a docking program's ability to predict the native pose of ligand. One important feature of this benchmarking set, as compared to the PDBBind Core set, is the inclusion of several cofactors such as zinc ions, and heme groups in the binding sites. Thus, to perform well on this benchmarking set, one must properly sample

ligand conformations interacting with metal ions and doing so requires adequate representation of metal-ligand interaction potentials at the atomic scale. To highlight the ability of our scoring function to characterize such interactions in a pair-wise fashion, we have produced plots for various atom pair interactions of interest to the medicinal chemistry in **Figure S13**.

Table 1 gives the number of complexes in this set where CANDOCK produces a ligand pose within 2.0 Å of the crystal pose. The success seen with CANDOCK on the Astex set can be attributed to the ability of our knowledge-based scoring functions to sample site of the given protein-ligand complexes.

For cases where cofactors interact with the ligand in a given complex, examples of CANDOCK successfully reproducing the crystal pose are given in **Figure 7** to showcase the versatility of the CANDOCK algorithm. In **Figure 7a-b** the energy minimization procedure moved the location of the Zn²⁺ ion in the binding pocket. This movement does not prevent the algorithm from producing a pose within 2.0 Å of the native pose and can be explained by the repulsive part of the minimization potential being too extreme (**Figure S13**). The docked pose of compounds that interact with a zinc ion through a sulfonyl amide group are shown in **Figure 7c-d**. For the compound in **Figure 7c**, the orientation of the sulfonyl amide aligns perfectly with the reference pose. For the compound in **Figure 7d**, the docked pose of the same group does not align with its reference; however, the overall pose still is within 2.0 Å of this reference. Therefore, the ability for CANDOCK to produce a pose within 2.0 Å of the reference is not dependent on correctly predicting the orientation of all functional groups in a given molecule.

The docking results where a larger organic cofactor is present in the binding site of the protein-ligand complex are given in **Figure 7e-h**. The heme group is present in several liver enzymes³⁹⁻⁴¹, therefore predicting the location of a ligand relative to this group is crucial to medicinal chemistry. **Figure 7e** demonstrates CANDOCK's ability to predict the pose of a compound relative to the heme group when the nitrogen of the compound is interacting with the iron atom of this group. A similar result is given **Figure 7f** where the interaction is between an aromatic carbon and the iron atom,

indicating that CANDOCK can reproduce the binding pose of a compound that interacts with a heme iron when the interacting atom is either of these atom types.

Producing a correct binding pose when a large cofactor is present is independent of the cofactor itself. This is shown for the flavin-adenine dinucleotide cofactor in **Figure 7g** where the dominate interaction between the ligand and the cofactor is π - π stacking. The ability to produce a good pose is still present when the type of interaction changes dramatically, as shown for the binuclear metal center formed by zinc and-magnesium in **Figure 7h**. This interaction is important for developing phosphodiesterase inhibitors⁴², therefore it is encouraging to observe CANDOCK's ability to produce a crystal pose in these cases. From these four case studies, we can conclude that CANDOCK is able to produce a reasonable docking pose in the presence of diverse cofactors.

CANDOCK also performs well with respect to other docking methodologies when benchmarked against using the Astex set. According to Gaudreault et al ¹⁶, there are four complexes in this set where Autdock Vina¹⁰, rDock¹⁵, FlexX⁴³, and FlexAID¹⁶ all have difficulty reproducing the crystal of the ligand. For these cases, CANDOCK is able to produce a crystal pose. This cases, along with their corresponding interactions are given in **Figure S9**.

3.6. Long distance cutoffs and a complete atom type set are needed to correlate RMSD and the knowledge-based score

A second, but also necessary, feature of a scoring function is its ability to correlate numerically with the RMSD of all generated poses for a ligand. This property is paramount when the scoring function is used to perform energy minimization calculations as a decrease in score should correspond to a decrease in RMSD. Therefore, we must justify the use of the objective function based on the RMC15 scoring function as the default objective function to use during energy minization.

To do so, we calculated the correlation between score and RMSD for all protein-ligand complexes in the PDBbind Core set. **Table S1** gives the average and median Pearson correlation values

between score and ligand RMSD taken over the entire PDBbind Core set for all scoring functions. For all scoring function families, increasing the cutoff distance from 4 Å to 15 Å corresponds to an increase in the correlation between RMSD and score. Additionally, ‘complete’ scoring functions have a superior correlation to RMSD than ‘reduced’ scoring functions and ‘mean’ scoring functions outperform their ‘cumulative’ counterparts. There is little difference between ‘radial’ and ‘normalized frequency’ scoring functions.

These averages indicate a relatively good correlation between score and RMSD for our chosen scoring function (RMC15) for use in the energy minimization procedure. Further, it is interesting to note that the median and average of these correlation values are relatively similar, indicating the distribution of correlation values are not biased towards high or low correlations for any given protein. In addition to this, the RMC15 score of the crystal pose have a strong correlation with the RMC15 score of the lowest RMSD pose (**Figure S6**) Additionally, the RMC15 score correlates well with the RMSD of the crystal pose(**Figure S7-8**). Therefore, we can conclude that RMC15 is the best choice for use in calculating the intermolecular forces during the energy minimization procedure.

3.7. Flexibility and knowledge of the crystal pose play minor roles in ranking the relative activity of a ligand

Another critical aspect of the scoring function we investigated is the ability to accurately rank the relative binding affinities of known binders to the same protein target. The PDBbind Core set provides experimental binding affinities and 3D coordinates of 5 protein- ligand complexes for each protein target. This allowed us to determine if a correlation exists between the measured binding affinities for each native ligand pose and our calculated docking score for that pose.

In this process we discovered that our best scoring function for selecting the crystal pose, RMR6, was not adequate at correlating its numeric score with the pKi/pKd values supplied by PDBbind. Upon further investigating, we discovered that using one scoring function to select the

representative pose of a complex and a second scoring function to rank the different cocrystals in order of binding affinity was the best way to obtain good correlation between score and pKi/pKd. This scheme is given in **Figure 8**.

The data presented in **Figure 9** shows the relationship between selecting the pose with various scoring functions and ranking the selected pose with a second scoring function (see **Figure S9** for details). There is little difference between the worst crystal pose selector (RCC11, **Figure 8c**) and the best selector (RMR6, **Figure 9d**). Therefore the ability of a selector to find the crystals pose of the ligand is not as important as the ranker.,. Further, the correlation between the RMC15 score and the pKi of a compound for all possible selectors (given in **Figure 9e**) does not deviate greatly, revealing that the selection of the pose for a co-crystal has a minor impact on ranking the activity of the ligand. This conclusion is further supported by **Figures S10-14** which show that difference between selecting a pose using RMR6 vs selecting the best RMSD pose does not improve ability to rank the pKi of compounds binding to the same protein when using RMC15 to rank the co-crystals. While these findings are encouraging as their remove the burden of finding the crystal pose of the ligand, a more in depth study using an additional benchmarking set such as the Directory of Useful Decoys (DUD-E)⁴⁴ is required to determine the proper choice of scoring function and protein target for complexes where the 3D coordinates are not provided.

An interesting observation is that the RMC15 score of weak binders (pKi < 2.5) does not correlate with the remainder of the poses (**Figure 9c-d**). Therefore, RMC15 may incorrectly score a low binding compound as a high binding one. This issue requires further investigation into our scoring function and its ability to rank the activity of protein-ligand complexes and discriminate decoys from actives.

Similar to the selector used, the flexibility mode used to generate ligand poses does not have a significant impact on the correlation between score and binding affinity (see **Figure 9f**). While the fully-flexible methodology has a significant advantage for the kinases ABL1, JAK2, and CHK1,

(**Figure S12**) there are few other examples where the fully-flexible method provides a clear advantage over the semi-flexible and rigid methodologies (**Figures S10** and **S11**). Again, this is significant because these methods are less computationally demanding than the fully-flexible method and can be used quickly in a virtual screen pipeline.

The correlation between score and pKi are different for the protein targets in question. For example, nuclear hormone receptors ER and AR have positive correlation values instead of the expected negative ones. In addition, the best selector/ranker pair for HIV proteases in the PDBbind core set is RMC15/RMR6 which is the opposite pair for all proteins in general. Therefore, the use of different scoring function may be advantageous in ranking the relative binding affinity of given ligands to the protein targets in a particular class of proteins.

4. Summary and Conclusions

In this work, we have presented CANDOCK, our hierarchal docking algorithm for quickly generating thousands of chemically relevant ligand poses utilizing our knowledge-based scoring functions. We have demonstrated these scoring functions are good for selecting a representative docked pose and ligands according to their measured pKd. Our methodology generates a docked ligand hierarchically by generating ligand fragments in a protein's binding pocket using an atomic grid and a pair-wise knowledge-based scoring to select the best-docked poses of the ligand fragments. These ligand fragments are linked together using fast graph theory algorithms to create a large number of chemically relevant potential ligand conformations in the target protein leading to a thorough sampling of the ligand's conformational space. Energy minimization procedures are used to give the protein flexibility during this linking procedure.

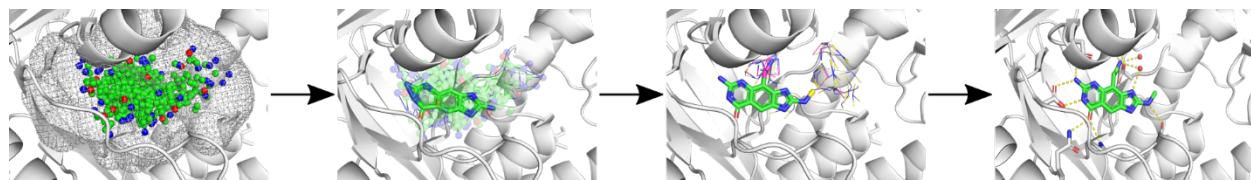
We conclude that only the final energy minimization is required to yield adequate sampling of this conformational space as defined by the method's ability to produce a pose within 2.0Å of the crystal binding pose for ligands consisting of more than six fragments. Our methodology performs

well even when cofactors are present in the binding site.

Further, we have shown that our knowledge-based scoring function using a short distance cutoff and reduced atom type set is adequate for selecting the crystal pose of the ligand, but a longer distance cutoff and complete atom type set are required to achieve reasonable correlation between RMSD and docking score. Similarly, a long cutoff and complete composition is required to obtain reasonable correlation between score and activity.

Finally, the use of the lowest RMSD pose vs. the best score pose does not make a substantial difference in ranking the relative strength of binding for a ligand to a single protein of interest, allowing one to use the relatively inexpensive semi-flexible method for the generation of ligand poses. We believe that the release of this code under the GPL license will give the community a valuable tool for generating chemically relevant ligand poses for use in drug discovery efforts as the codebase is developed in a modular manner so that it can be embedded in drug-design pipelines.

Figures and captions



Abstract Figure

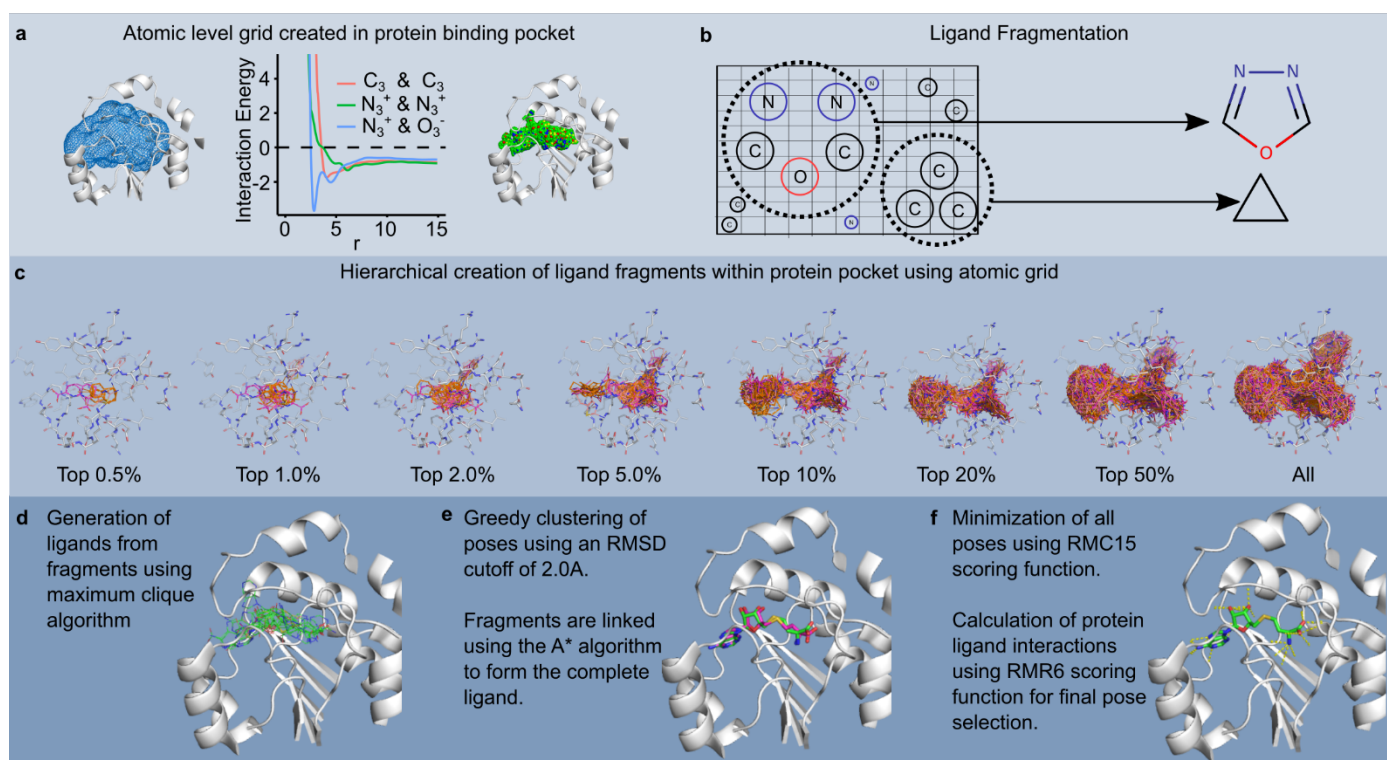


Figure 1: Overview of the CANDOCK docking algorithm. Phase I consists of processing the input protein (**a**) and the ligand (**b**). During this Phase, an atomic grid is created in the protein binding site where the scores of all possible atom types at each point in the binding site grid. Simultaneously, the input ligand(s) are fragmented along the rotatable bonds present in the ligand. The grid is used to recreate the rigid fragments in the binding pocket. (**c**) Phase II constructs the rigid ligand fragments in the binding site grid producing ‘seeds’ that can be grown into the full ligand. Phase III identifies potential ligand poses using maximum clique (**d**), clusters and links these poses using A* (**e**) and minimizes the poses into the binding site (**f**).

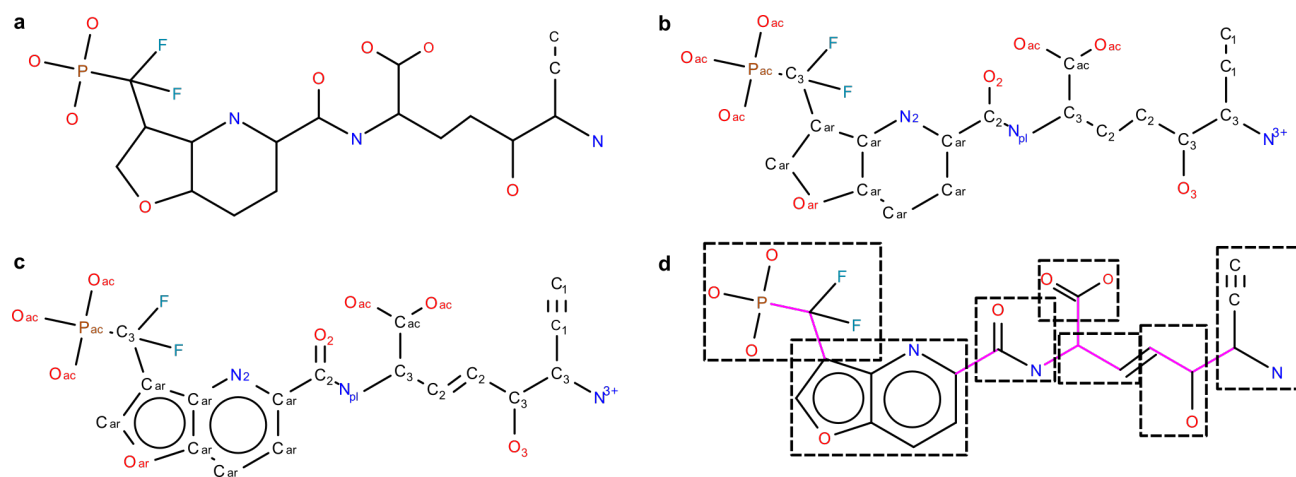


Figure 2: (a) Atom type assignment and fragmentation procedure present in CANDOCK. The procedure begins with the topology and 3D coordinates of the ligand. (b) Using these data, the IDATM type is assigned to each atom in the ligand using a previously described algorithm²⁷. (c) This yields the hybridization state of all atoms, allowing for the assignment of bond orders for all atoms. (d) The bond orders and topologies are used to assign a rotatable flag for each bond in the ligand using rules derived from the DOCK 6 program³¹. The rigid fragments identified using this method are boxed..

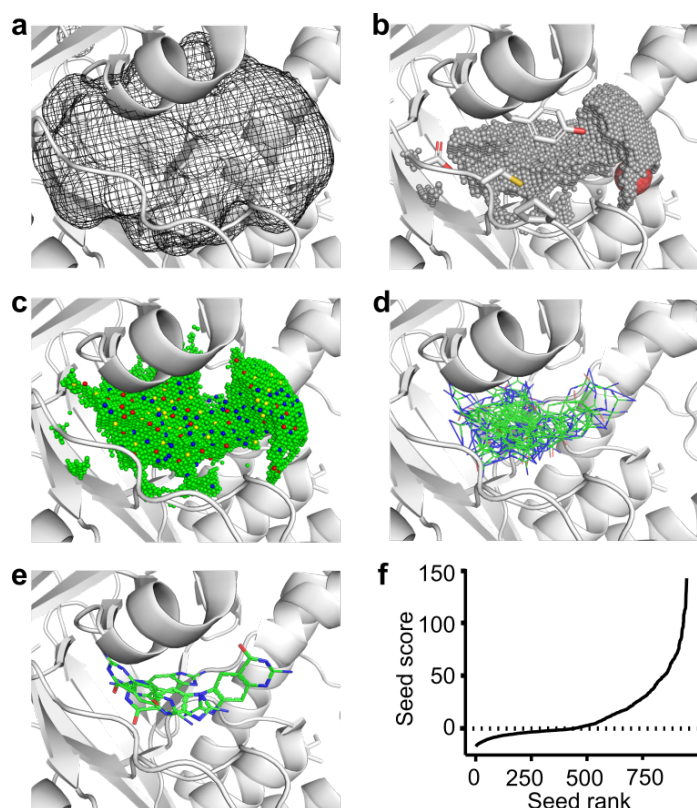


Figure 3: Detailed overview of the hierarchal relationship between the atomic grid and ligand fragments. The protein binding site is supplied as a series of centroids that are combined to form a volume of space that defines the binding pocket (**a**). Regions of this volume that do not clash with the protein, waters, or cofactors are filled with a hexagonal close-packed grid (**b**). The score of all atom types present in the ligand are calculated at each grid point using the RMR6 scoring function (**c**). Ligand fragments from the previous step are translated and rotated within this grid to produce a collection of the same ligand fragment throughout the binding site (**d**). This collection of ligand fragments is clustered using a greedy clustering algorithm using RMSD to determine if two fragments are similar. If two fragments are within a 2.0Å of each other, the fragment with a higher RMR6 is deleted. Remaining docked fragments are referred to as seeds (**e**). The score distribution of a typical seed is given in (**f**) to show the exponential score shape of the distribution.

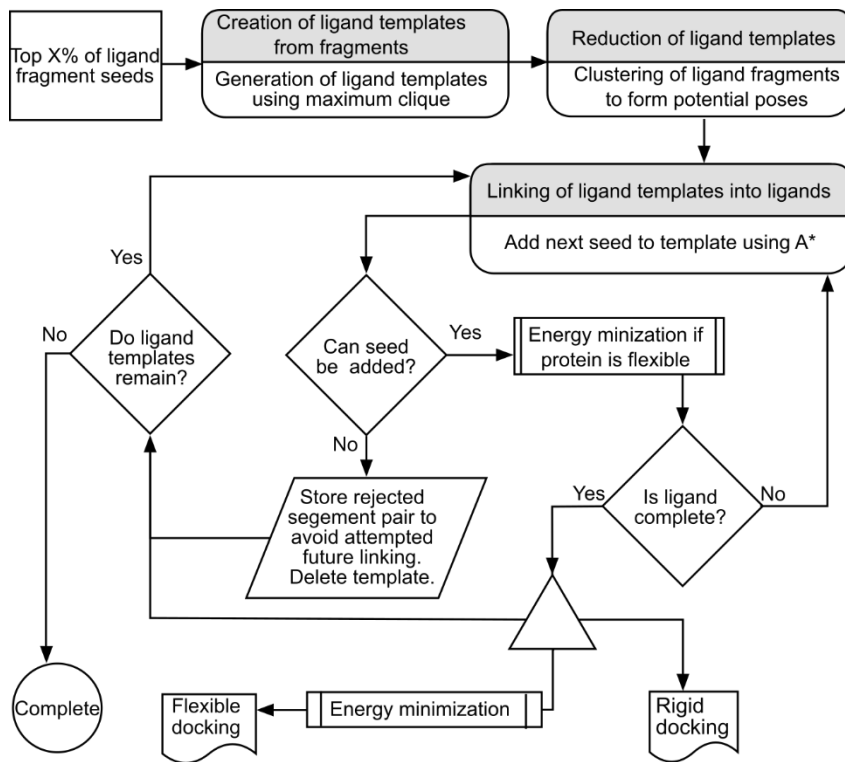


Figure 4: Workflow of the fragment linking procedure.

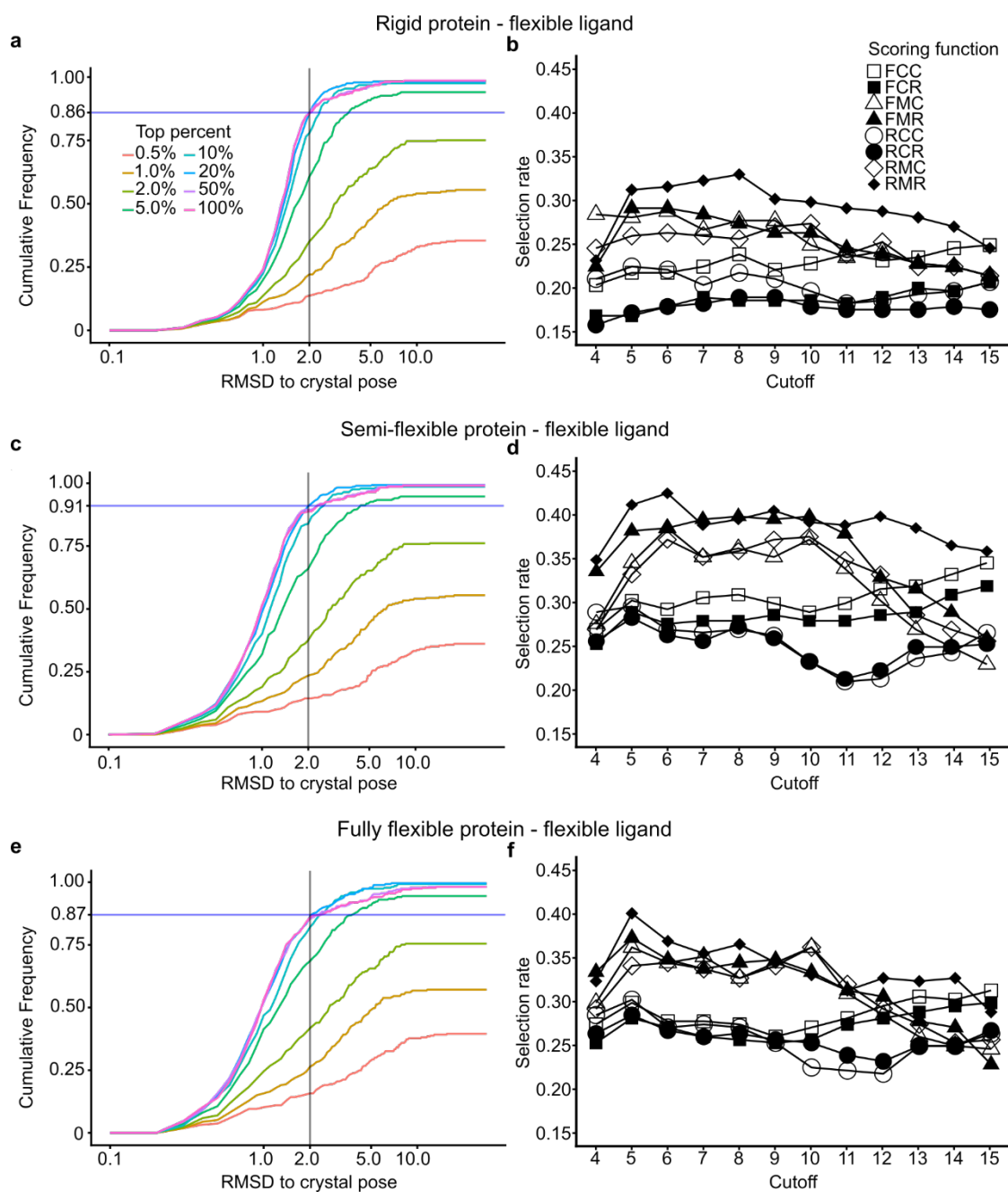


Figure 5: Cumulative frequency plots for rigid (no energy minimization), semi-flexible (energy minimization at the end), and fully-flexible (iterative energy minimization during linking procedure) CANDOCK docking results are given in (a), (c), and (e) respectively. The selection rate, i.e., portion of the best-scored docked poses within 2.0 Å of the native, is given for different scoring functions employed in (b), (d), and (f).

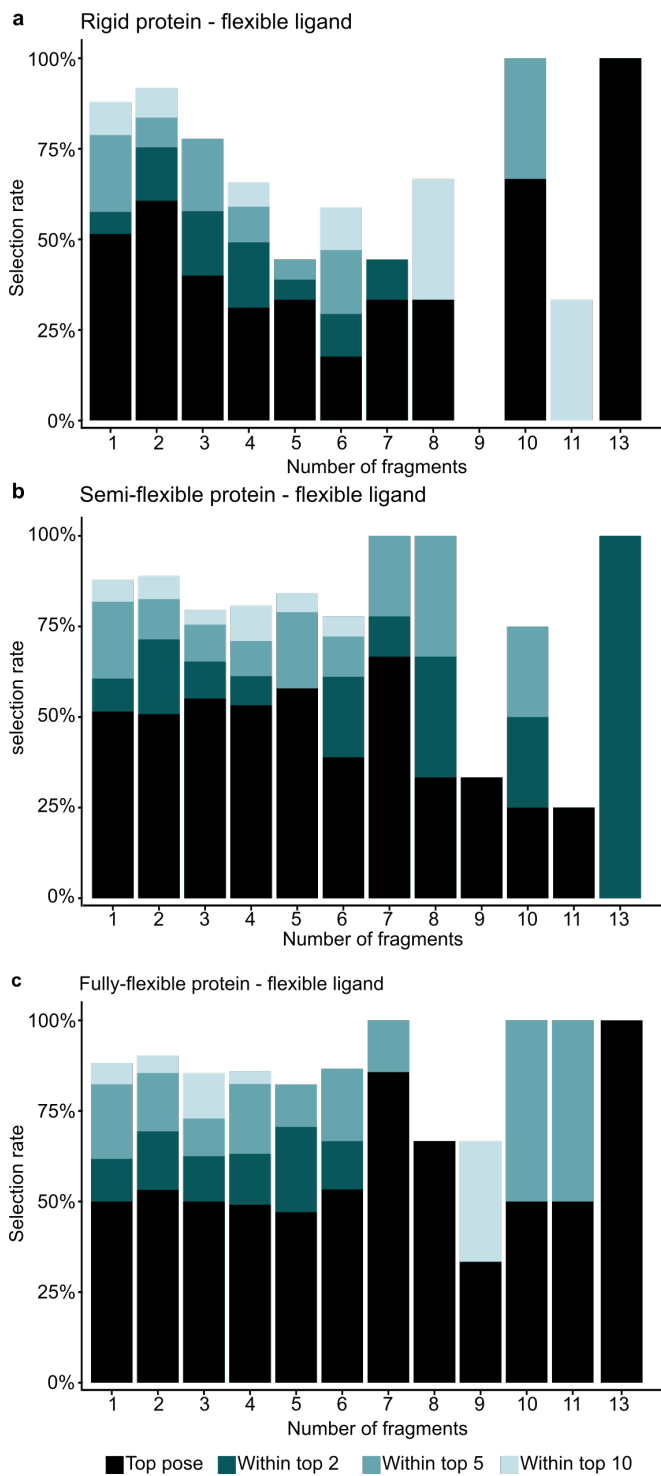
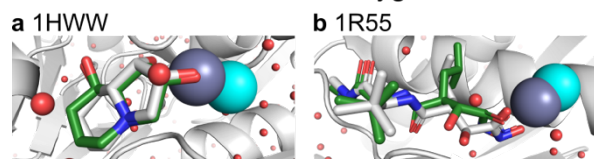
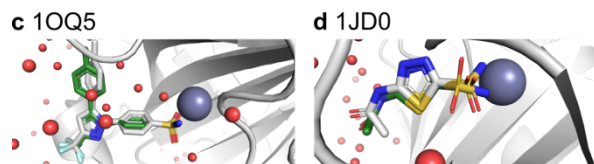


Figure 6: Selection rates for the RMR6 scoring function with rigid (a), semi-flexible (b), and fully-flexible (c) CANDOCK docking arranged by the numbers of ligand fragments in the PDBbind core set (see Figure 2 for the definition of a fragment).

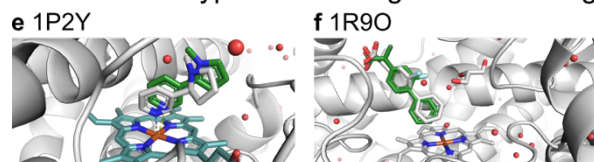
Interactions between SP² oxygen and zinc



Interactions between a sulfamide group and zinc



Various atom types interacting with a Heme group



Other ligand-cofactor interactions

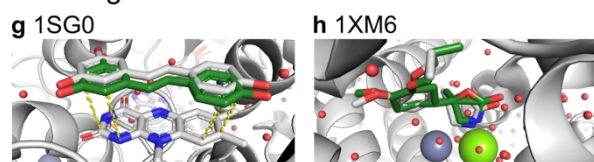


Figure 8: Example docked ligand poses from the Astex Diverse set that show versatility of the CANDOCK algorithm in handling cofactors. In all panels, the reference pose is given in white and the lowest RMSD pose predicted by CANDOCK with a ‘Top Percent’ value of 20% using the semi-flexible method is given in green. Panels (a) and (b) were selected due to presence of oxygen-zinc interactions between native ligand and protein. The zinc ion before and after energy minimization is given in gray and cyan respectively showing that the energy minimization moved the zinc ion considerably. The complexes in (c) and (d) show the interactions between sulfonyl amide groups and a zinc ion. The interactions of a compound with a heme group via a nitrogen lone pair is shown in (e) and the interaction of an aromatic carbon with a heme group is given in (f). Finally, panels (g) and (h) show the interactions of compounds with other cofactors, such as a π - π interaction of a compound with flavin-adenine dinucleotide and interaction of a compound with zinc and magnesium in a binding pocket.

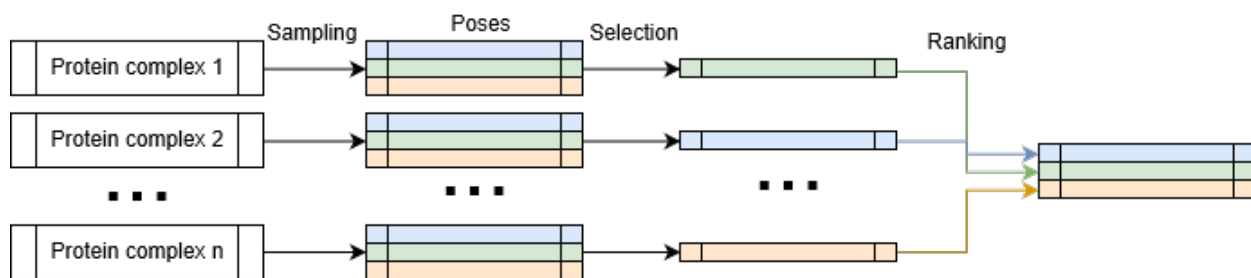


Figure 8: CANDOCK activity evaluation pipeline. Sampling is performed using the RMR6 scoring function to generate thousands of ligand poses. The best pose is selected with a ‘selector’ scoring function to represent the protein-ligand complex. Only this selected pose is rescored using the ‘ranker’ scoring function, which is used to assign a new score to the complex. This score is compared to other scores obtained from other complexes to rank the complex in terms of pKd.

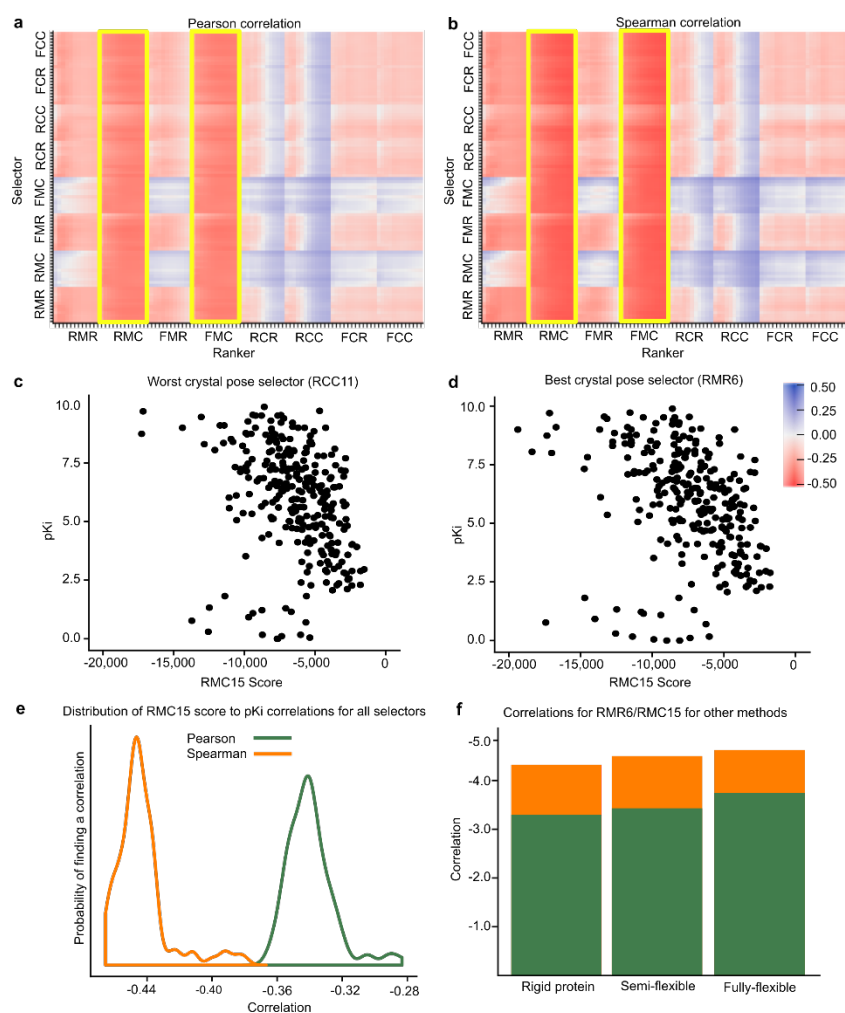


Figure 9: The Pearson (a) and Spearman (b) correlation coefficients between all pairs of selector and ranker scoring functions (arranged by family) and the experimental pKi of any complexes in the PDBbind Core set. The RMC and FMC (highlighted in yellow) families perform best and there is a general trend where an increase in cutoff (from left to right) results in improved performance in ranking complexes in order of their measured pKi. Plots of pKi vs RMC15 score are given in (c) and (d) for the worst crystal pose selector (RCC11) and the best crystal pose selector (RMR6), respectively. The lack of major differences between these two selectors with the same ranker indicates the lack of importance in selecting the correct binding pose for ranking the pKi of a protein-ligand complex. (e) The distribution of all correlations, regardless of selector, for the RMC15 scoring function. (f) The correlations for other docking methods with RMR6 as the selector and RMC15 as the ranker.

TOP PERCENT	RIGID PROTEIN	SEMI-FLEXIBLE PROTEIN
0.5%	7	7
1.0%	14	15
2.0%	28	33
5.0%	57	60
10%	67	74
20%	77	79
50%	79	82
100%	78	81
ALL POSES	81	83

Table 1. Number of successes in the Astex diverse Set for all ‘Top Percent’ values investigated. There is a total of 85 protein-ligand complexes in this benchmarking set.

References

- (1) Warren, G. L.; Andrews, C. W.; Capelli, A. M.; Clarke, B.; LaLonde, J.; Lambert, M. H.; Lindvall, M.; Nevins, N.; Semus, S. F.; Senger, S.; et al. A Critical Assessment of Docking Programs and Scoring Functions. *J. Med. Chem.* **2006**, *49* (20), 5912–5931.
- (2) Kellenberger, E.; Rodrigo, J.; Muller, P.; Rognan, D. Comparative Evaluation of Eight Docking Tools for Docking and Virtual Screening Accuracy. *Proteins Struct. Funct. Bioinforma.* **2004**, *57* (2), 225–242.
- (3) Bissantz, C.; Bernard, P.; Hibert, M.; Rognan, D. Protein-Based Virtual Screening of Chemical Databases. II. Are Homology Models of G-Protein Coupled Receptors Suitable Targets? *Proteins Struct. Funct. Bioinforma.* **2002**, *50* (1), 5–25.
- (4) Niu Huang; Brian K. Shoichet, * and; Irwin*, J. J. Benchmarking Sets for Molecular Docking. **2006**.
- (5) Wang, Z.; Sun, H.; Yao, X.; Li, D.; Xu, L.; Li, Y.; Tian, S.; Hou, T. Comprehensive Evaluation of Ten Docking Programs on a Diverse Set of Protein-Ligand Complexes: The Prediction Accuracy of Sampling Power and Scoring Power. *Phys. Chem. Chem. Phys.* **2016**, *18*, 12964–12975.
- (6) Claußen, H.; Buning, C.; Rarey, M.; Lengauer, T. FLEXE: Efficient Molecular Docking Considering Protein Structure Variations. *J. Mol. Biol.* **2001**, *308* (2), 377–395.
- (7) Leach, A. R. Ligand Docking to Proteins with Discrete Side-Chain Flexibility. *J. Mol. Biol.* **1994**, *235* (1), 345–356.
- (8) Ding, F.; Yin, S.; Dokholyan, N. V. Rapid Flexible Docking Using a Stochastic Rotamer Library of Ligands. *J. Chem. Inf. Model.* **2010**, *50* (9), 1623–1632.
- (9) Apostolakis, J.; Plückthun, A.; Caflisch, A. Docking Small Ligands in Flexible Binding Sites. *J. Comput. Chem.* **1998**, *19* (1), 21–37.
- (10) Trott, O.; Olson, A. J. AutoDock Vina: Improving the Speed and Accuracy of Docking with a New Scoring Function, Efficient Optimization, and Multithreading. *J. Comput. Chem.* **2010**, *31* (2), 455–461.
- (11) Meng, E. C.; Gschwend, D. A.; Blaney, J. M.; Kuntz, I. D. Orientational Sampling and Rigid-Body Minimization in Molecular Docking. *Proteins Struct. Funct. Genet.* **1993**, *17* (3), 266–278.
- (12) Zhao, H.; Caflisch, A. Discovery of ZAP70 Inhibitors by High-Throughput Docking into a Conformation of Its Kinase Domain Generated by Molecular Dynamics. *Bioorg. Med. Chem. Lett.* **2013**, *23* (20), 5721–5726.
- (13) Zavodszky, M. I.; Kuhn, L. A. Side-Chain Flexibility in Protein-Ligand Binding: The Minimal Rotation Hypothesis. *Protein Sci.* **2005**, *14* (4), 1104–1114.
- (14) Chen, Y. C. Beware of Docking! *Trends Pharmacol. Sci.* **2015**, *36* (2), 78–95.
- (15) Ruiz-Carmona, S.; Alvarez-Garcia, D.; Foloppe, N.; Garmendia-Doval, A. B.; Juhos, S.; Schmidtke, P.; Barril, X.; Hubbard, R. E.; Morley, S. D. RDock: A Fast, Versatile and Open Source Program for Docking Ligands to Proteins and Nucleic Acids. *PLoS Comput. Biol.* **2014**, *10* (4).
- (16) Gaudreault, F.; Najmanovich, R. J. FlexAID: Revisiting Docking on Non-Native-Complex Structures. *J. Chem. Inf. Model.* **2015**, *55* (7), 1323–1336.
- (17) Nedumpully-Govindan, P.; Jemec, D. B.; Ding, F. CSAR Benchmark of Flexible MedusaDock in Affinity Prediction and Nativelike Binding Pose Selection. *J. Chem. Inf. Model.* **2016**, *56* (6), 1042–1052.
- (18) Verdonk, M. L.; Cole, J. C.; Hartshorn, M. J.; Murray, C. W.; Taylor, R. D. Improved Protein-Ligand Docking Using GOLD. *Proteins Struct. Funct. Bioinforma.* **2003**, *52* (4), 609–623.
- (19) Carlson, H. A.; Smith, R. D.; Damm-Ganamet, K. L.; Stuckey, J. A.; Ahmed, A.; Convery, M.

- A.; Somers, D. O.; Kranz, M.; Elkins, P. A.; Cui, G.; et al. CSAR 2014: A Benchmark Exercise Using Unpublished Data from Pharma. *J. Chem. Inf. Model.* **2016**, *56* (6), 1063–1077.
- (20) Onodera, K.; Satou, K.; Hirota, H. Evaluations of Molecular Docking Programs for Virtual Screening. *J. Chem. Inf. Model.* **2007**, *47* (4), 1609–1618.
- (21) Feher, M.; Williams, C. I. Effect of Input Differences on the Results of Docking Calculations. *J. Chem. Inf. Model.* **2009**, *49* (7), 1704–1714.
- (22) Pevzner, Y.; Frugier, E.; Schalk, V.; Caflisch, A.; Woodcock, H. L. Fragment-Based Docking: Development of the CHARMMing Web User Interface as a Platform for Computer-Aided Drug Design. *J. Chem. Inf. Model.* **2014**, *54* (9), 2612–2620.
- (23) Belew, R. K.; Forli, S.; Goodsell, D. S.; O'Donnell, T. J.; Olson, A. J. Fragment-Based Analysis of Ligand Dockings Improves Classification of Actives. *J. Chem. Inf. Model.* **2016**, *56* (8), 1597–1607.
- (24) Vilar, S.; Cozza, G.; Moro, S. Medicinal Chemistry and the Molecular Operating Environment (MOE): Application of QSAR and Molecular Docking to Drug Discovery. *Curr. Top. Med. Chem.* **2008**, *8* (18), 1555–1572.
- (25) Freire, I. L. and E. Structural Stability of Binding Sites: Consequences for Binding Affinity and Allosteric Effects. *Proteins Struct. Funct. Genet.* **2000**, *4*, 63–71.
- (26) Bernard, B.; Samudrala, R. A Generalized Knowledge-Based Discriminatory Function for Biomolecular Interactions. *Proteins Struct. Funct. Bioinforma.* **2009**.
- (27) Meng, E. C.; Lewis, R. A. Determination of Molecular Topology and Atomic Hybridization States from Heavy Atom Coordinates. *J. Comput. Chem.* **1991**, *12* (7), 891–898.
- (28) Wang, J.; Wolf, R. M.; Caldwell, J. W.; Kollman, P. A.; Case, D. A. Development and Testing of a General Amber Force Field. *J. Comput. Chem.* **2004**, *25* (9), 1157–1174.
- (29) Wang, J.; Wang, W.; Kollman, P. A.; Case, D. A. Automatic Atom Type and Bond Type Perception in Molecular Mechanical Calculations. *J. Mol. Graph. Model.* **2006**, *25* (2), 247–260.
- (30) Eastman, P.; Swails, J.; Chodera, J. D.; McGibbon, R. T.; Zhao, Y.; Beauchamp, K. A.; Wang, L.-P.; Simmonett, A. C.; Harrigan, M. P.; Stern, C. D.; et al. OpenMM 7: Rapid Development of High Performance Algorithms for Molecular Dynamics. *PLOS Comput. Biol.* **2017**, *13* (7), e1005659.
- (31) Allen, W. J.; Balius, T. E.; Mukherjee, S.; Brozell, S. R.; Moustakas, D. T.; Lang, P. T.; Case, D. A.; Kuntz, I. D.; Rizzo, R. C. DOCK 6: Impact of New Features and Current Docking Performance. *J. Comput. Chem.* **2015**, *36* (15), 1132–1156.
- (32) Groom, C. R.; Bruno, I. J.; Lightfoot, M. P.; Ward, S. C.; IUCr. The Cambridge Structural Database. *Acta Crystallogr. Sect. B Struct. Sci. Cryst. Eng. Mater.* **2016**, *72* (2), 171–179.
- (33) Rose, P. W.; Prlić, A.; Bi, C.; Bluhm, W. F.; Christie, C. H.; Dutta, S.; Green, R. K.; Goodsell, D. S.; Westbrook, J. D.; Woo, J.; et al. The RCSB Protein Data Bank: Views of Structural Biology for Basic and Applied Research and Education. *Nucleic Acids Res.* **2015**, *43* (D1), D345–D356.
- (34) Konc, J.; Janežič, D. An Improved Branch and Bound Algorithm for the Maximum Clique Problem. *MATCH Commun. Math. Comput. Chem.* **2007**, *58*, 569–590.
- (35) Liu, D. C.; Nocedal, J. On the Limited Memory BFGS Method for Large Scale Optimization. *Math. Program.* **1989**, *45* (1–3), 503–528.
- (36) Liu, Z.; Su, M.; Han, L.; Liu, J.; Yang, Q.; Li, Y.; Wang, R. Forging the Basis for Developing Protein-Ligand Interaction Scoring Functions. *Acc. Chem. Res.* **2017**, *50* (2), 302–309.
- (37) Hartshorn, M. J.; Verdonk, M. L.; Chessari, G.; Brewerton, S. C.; Mooij, W. T. M.; Mortenson, P. N.; Murray, C. W. Diverse, High-Quality Test Set for the Validation of Protein-Ligand Docking Performance. *J. Med. Chem.* **2007**.
- (38) Nivedha, A. K.; Thieker, D. F.; Makeneni, S.; Hu, H.; Woods, R. J. Vina-Carb: Improving

- Glycosidic Angles during Carbohydrate Docking. *J. Chem. Theory Comput.* **2016**, *12* (2), 892–901.
- (39) Bezhentsev, V. M.; Tarasova, O. A.; Dmitriev, A. V; Rudik, A. V; Lagunin, A. A.; Filimonov, D. A.; Poroikov, V. V. Computer-Aided Prediction of Xenobiotic Metabolism in the Human Body. *Russ. Chem. Rev.* **2016**, *85* (8), 854–879.
- (40) Kirchmair, J.; Göller, A. H.; Lang, D.; Kunze, J.; Testa, B.; Wilson, I. D.; Glen, R. C.; Schneider, G. Predicting Drug Metabolism: Experiment and/or Computation? *Nature Reviews Drug Discovery*. 2015.
- (41) Kirchmair, J.; Williamson, M. J.; Tyzack, J. D.; Tan, L.; Bond, P. J.; Bender, A.; Glen, R. C. Computational Prediction of Metabolism: Sites, Products, SAR, P450 Enzyme Dynamics, and Mechanisms. *Journal of Chemical Information and Modeling*. 2012.
- (42) Card, G. L.; England, B. P.; Suzuki, Y.; Fong, D.; Powell, B.; Lee, B.; Luu, C.; Tabrizizad, M.; Gillette, S.; Ibrahim, P. N.; et al. Structural Basis for the Activity of Drugs That Inhibit Phosphodiesterases. *Structure* **2004**, *12* (12), 2233–2247.
- (43) Cross, S. S. J. Improved FlexX Docking Using FlexS-Determined Base Fragment Placement. *J. Chem. Inf. Model.* **2005**, *45* (4), 993–1001.
- (44) Mysinger, M. M.; Carchia, M.; Irwin, J. J.; Shoichet, B. K. Directory of Useful Decoys, Enhanced (DUD-E): Better Ligands and Decoys for Better Benchmarking. *J. Med. Chem.* **2012**, *55* (14), 6582–6594.